Cold Regions Science and Technology 171 (2020) 102958

Contents lists available at ScienceDirect

Cold Regions Science and Technology

journal homepage: www.elsevier.com/locate/coldregions

Snow liquid water content measurement using an open-ended coaxial probe (OECP)

Alex Mavrovic[a,b,c,*], Jean-Benoit Madore[a,b], Alexandre Langlois[a,b], Alain Royer[a,b], Alexandre Roy[c,b]

[a] Centre d'Applications et de Recherches en Télédétection, Université de Sherbrooke, Sherbrooke, Québec J1K 2R1, Canada
[b] Centre d'Études Nordiques, Université Laval, Québec G1V 0A6, Canada
[c] Université du Québec à Trois-Rivières, Trois-Rivières, Québec G9A 5H7, Canada

ARTICLE INFO

Keywords:
Open-ended coaxial probe
Snow liquid water content
Avalanche risk assessment
Microwave snow observations
Snow microwave permittivity

Abstract: Accurately determining the evolution of the snow liquid water content (LWC) through the snowpack remains a challenge in avalanche risk assessment and microwave snow emission and backscattering modeling. The percolation of rain and/or snowmelt water can lead to instability in the snowpack and increase avalanche risk. Liquid water percolation schemes have recently been integrated into snow metamorphism models, but they require validation. Snow property retrievals from microwave observations (satellite and ground-based) are challenging in wet snow conditions because of the reduced penetration depth, and thus a better quantification of the effect of snow liquid water content on microwave signals would improve satellite products. This study presents a new open-ended coaxial probe (OECP) suitable for in situ snow LWC measurements at L-band frequencies (1–2 GHz). The precision of ± 1% of the OECP compared to calorimetric measurements is similar to other available instruments tested (Snow Fork and Time Domain Reflectometry). The OECP is capable of quantifying the LWC of thin percolation accumulation layers because of its small probed volume, while other instruments fail to do because of their bigger probed volume due to their lower frequencies used.

1. Introduction

Precise snow state variable measurement has been consistently improved over the years to the point where it now provides rapid and reliable information on snow microstructure and other related geophysical properties. Among these variables, liquid water content (hereinafter, LWC will describe volumetric snow liquid water content) in snow represents an important metric for the evaluation of various dynamic and thermodynamic processes in the snowpack. The percolation of water from rain and/or snowmelt can lead to instability in the snowpack through the additional weight of wet snow, the reduction of snow cohesion and the accumulation of water at capillary barriers (Mitterer et al., 2011a). The understanding of these instabilities through percolation schemes in layered snow as well as their detection is essential for improving avalanche risk assessment (Wever et al., 2014; Wever et al., 2016a). Ice crusts have also proven to have a negative impact on ungulate grazing conditions in the Arctic (Dolant et al., 2018), while lingering uncertainties remain with regards to the impact of percolation and preferential flow on freeze/thaw cycles throughout the cryosphere given the enhanced thermal conductivity (Barrere et al., 2018) and metamorphism (Dominé et al., 2008; Morin et al., 2010) of wet snow. Despite a growing understanding of the impact of water on the air-snow-soil interface, very limited progress has been made in simulating snow liquid water content and transport within the snowpack owing to the difficulty of measuring such variables. With the recent integration of new percolation schemes in multi-layered snow models (Wever et al., 2014; D'Amboise et al., 2017) and the evaluation of modeled preferential flow (Wever et al., 2016b), precise measurements of the vertical variability and accumulation of LWC in snowpack are needed for the validation and the implementation of models, which can then be used for global assessments of soil thermal regimes, hydrological cycles, ecological processes and avalanche risk.

Of particular relevance, given the great sensitivity of brightness temperatures to LWC (though dielectric properties), passive microwave remote sensing (Mätzler et al., 2006; Mätzler and Wiesmann, 2007; Roy et al., 2017) has been used to show that the occurrence of rain-on-snow (ROS) events is increasing in Arctic regions (Dolant et al., 2017; Langlois et al., 2017). Recently, satellite and ground-based remote sensing of the snowpack via microwave devices have been put forward to retrieve snowpack state, such as snow liquid water content and snow

* Corresponding author at: Centre d'Applications et de Recherches en Télédétection, Université de Sherbrooke, Sherbrooke, Québec J1K 2R1, Canada.
E-mail address: Alex.Mavrovic@USherbrooke.ca (A. Mavrovic).

https://doi.org/10.1016/j.coldregions.2019.102958
Received 27 April 2019; Received in revised form 22 November 2019; Accepted 30 November 2019
Available online 04 December 2019
0165-232X/

water equivalent (Naderpour and Schwank, 2018; Pérez Diaz et al., 2017; Schmid et al., 2016; Mitterer et al., 2011a; Takala et al., 2011). Precise LWC measurements are required to take into account the effect of LWC on radiative transfer models in order to improve microwave (passive and active) satellite products. Snow permittivity being frequency dependent, direct measurements of 1.4 GHz snow permittivity would also be useful for validation and improvement freeze/thaw products from L-band satellite-based radiometers launched over the last decade: the NASA Soil Moisture Active Passive mission (SMAP; Entekhabi et al., 2010; Derksen et al., 2017), the European Space Agency Soil Moisture Ocean Salinity mission (SMOS; Kerr et al., 2010; Rautiainen et al., 2016) and the NASA/CONAE (Comisión Nacional de Actividades Espaciales) joint Aquarius mission (Le Vine et al., 2010; Prince et al., 2018).

Field instruments for measuring the vertical variability of LWC in snowpack have been developed since the 1980's. They generally measure the dielectric component of the snow at wavelengths between 10 MHz and 1 GHz. The Finnish Snow Fork (Sihvola and Tiuri, 1986) and the Denoth instrument (Denoth, 1994) are devices commonly used for LWC measurements. Techel and Pielmeier (2011) made extensive measurements with those instruments and showed a good correspondence (± 1% of LWC). Nevertheless, developing new instruments and ways to improve LWC measurements is crucial to increase the quality and amount of data available to validate models and account for the various snow conditions to be sampled (i.e. alpine vs. Arctic snowpacks) that would benefit from different sample volumes. A new 1.4 GHz coaxial sensor was developed to measure the complex permittivity of vegetation (Mavrovic et al., 2018). This sensor has the potential for LWC retrieval in snow and was tested at two different sites in Canada: Glacier National Park (British Columbia, Canada) and the Université de Sherbrooke research station (Québec, Canada).

The goal of this study is thus to introduce and validate an L-band open-ended coaxial probe (OECP) used for the in situ measurements of LWC. The OECP infers LWC from snow permittivity measurements at the interface between the probe and the snow using a physically-based model. OECP performance was compared to three other available devices/methods. Section 2 discusses other available devices to measure LWC and the theory behind the OECP measurements. Section 3 provides context for the study sites and data collection. In section 4, the justification of the need for a physically-based model and how the OECP performance and precision compared with other available instruments are discussed.

2. Theoretical background

2.1. LWC measurement methods

There are two general approaches to measuring LWC: direct measurement and indirect measurement. The direct measurement methods include centrifugal separation, freezing calorimetry and melting calorimetry (Fig. 1a) (Stein et al., 1997). These methods require important material resources and are time-consuming. Therefore, they are difficult to implement in the field and more efficient indirect measurement methods are preferred. Indirect measurement uses the strong relationship between snow microwave permittivity (ε') and LWC since water permittivity is much higher than air and ice permittivity. Such indirect measurements of LWC use the empirical relationship with snow permittivity (Denoth et al., 1984; Denoth, 1989). Instruments that measure microwave snow permittivity include the Finnish Snow Fork (Sihvola and Tiuri, 1986) and the A2 Photonic Sensors' WISe resonator (A2 Photonic Sensors, 2019) (Fig. 1b and c). To our knowledge, other permittivity–based snow instruments were developed, but never became widely available such as the previously mentioned ones. Those instruments include Mätzler's resometer (Mätzler, 1996; Aebischer and Maetzler, 1983; Ulaby et al., 1986) and Kendra's snow probe (Kendra et al., 1994), both acting as resonators, and Time Domain Reflectometry consisting of measuring reflection along a conductor at low microwave frequency (MHz). (TDR) (Stein and Kane, 1983; Stein et al., 1997; Lundberg, 1997; Pérez Diaz et al., 2017).

In order to retrieve LWC from devices that measure permittivity, calorimetry measurements are used to calculate proper empirical calibration that relates permittivity to LWC. The open-ended coaxial probe also infers LWC from the measured permittivity but uses a physical model and assumes that the permittivity of water, ice and air at 1.4 GHz is known.

2.2. Calorimetry

Freezing and melting calorimetry can be used for LWC measurement. Freezing calorimetry consists of freezing the entire liquid water fraction of snow. The LWC is then determined by heat transfer between snow and the calorimeter's cold liquid (i.e. light silicon oil; Jones et al., 1983). Melting calorimetry operates on the same principle, but instead of freezing the snow water fraction, the snow ice fraction is melted using a hot liquid (i.e. hot water; Yosida, 1960). Since hot water was more readily available in the field than a cold antifreeze substance, melting calorimetry was used in this paper. The heat transfer formula for melting calorimetry derived from the conservation of energy (Eq.1).

$$-Q_{cal} = Q_{snow} \tag{1}$$

where Q_{cal} and Q_{snow} are respectively the heat transfer of the calorimeter hot liquid and snow (J). Snow is composed of ice, water and air. Because of its small mass, the heat transfer contribution of air was neglected in Eq. 2.

$$-Q_{cal} = Q_{water} + Q_{ice} \tag{2}$$

The contribution of each term is evaluated using the heat transfer definition (Eq. 3) and latent heat (Eq. 4).

$$Q_{transfer} = m \cdot c \bullet \Delta T \tag{3}$$

$$Q_{latent} = m \cdot L \tag{4}$$

where m is the mass (kg), c the heat specific capacity (J K^{-1} kg^{-1}), ΔT the temperature difference between the start and end of the heat transfer (K) and L the specific latent heat (J kg^{-1}). Knowing that the combined mass of water and ice equals the mass of snow (m_{snow}), Eq. 5 can be derived from Eq. 2, 3 and 4.

$$m_{water} = m_{snow} - \frac{m_{cal} \cdot c_{water} \cdot \Delta T_{cal \rightarrow eq} + m_{snow} \cdot c_{water} \cdot \Delta T_{snow \rightarrow eq}}{c_{ice} \cdot T_{snow} - L_{ice/water} - c_{water} \cdot T_{eq} + c_{water} \cdot \Delta T_{snow \rightarrow eq}} \tag{5}$$

where the index *cal* refer to the calorimeter's hot water, the index *water* the liquid water in the snow composition, *eq* the temperature at equilibrium after the snow was added to the calorimeter. The latent heat of the transition from ice to water and the heat specific capacity of both water and ice are well-known constants. All other parameters consist of masses and temperatures and are therefore measurable in the field. The gravimetric LWC is obtained by calculating the ratio of m_{water} to m_{snow}. The volumetric LWC can be calculated from snow density ρ_{snow} (g m^{-3}) with Eq. 6.

$$LWC(vol.) = LWC(mass) \cdot \frac{\rho_{snow}}{\rho_{water}} \tag{6}$$

2.3. Snow Fork

The Snow Fork, developed by the Finnish Meteorological Institute (Sihvola and Tiuri, 1986), is composed of two steel needles that act as a waveguide to measure the complex permittivity of snow (real and imaginary parts). It probes samples of snow within a cylindrical volume of about 2 × 7.5 cm and operates between 500 and 1000 MHz. This is an estimated probed area since snow characteristics affect probed

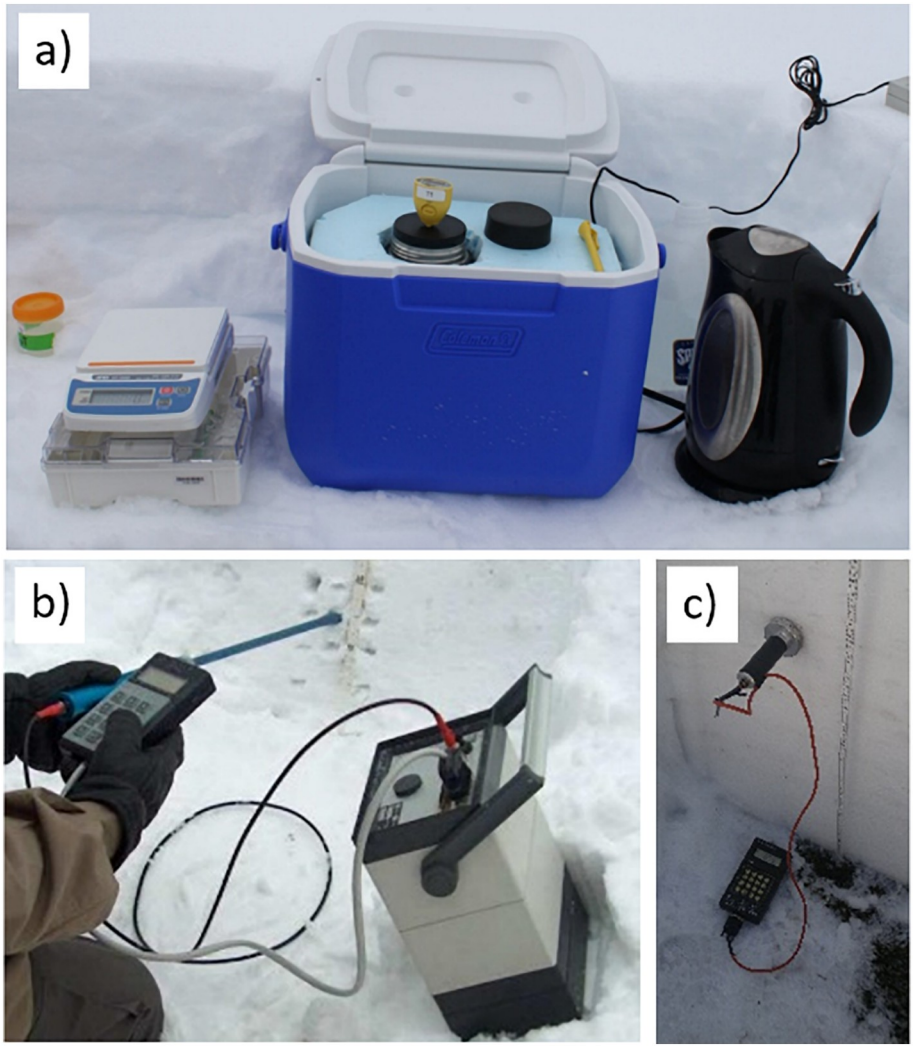

Fig. 1. LWC measurement methods: (a) Calorimeter, (b) Snow fork (Source: Toikka Engineering Ltd.) and (c) Early version of the WISe.

volume. For example, a higher LWC induces a higher snow permittivity, reducing the probed volume. To infer LWC and density from permittivity measurements, empirical equations based on freezing calorimetry measurements were developed (Tiuri et al., 1984). LWC is obtained with Eq. 7 from the imaginary part of snow permittivity.

$$\varepsilon_s'' = f \bullet (0.9LWC + 7.5LWC^2) \tag{7}$$

where ε_s'' is the imaginary part of snow permittivity (unitless) and f the frequency (GHz). Snow density is obtained with Eq. 8 and 9 from the real part of snow permittivity and LWC.

$$\varepsilon_s' = 1 + 1.7\frac{\rho_d}{\rho_w} + 0.7\left(\frac{\rho_d}{\rho_w}\right)^2 + 8.7LWC + 70LWC^2 \tag{8}$$

$$\frac{\rho_s}{\rho_w} = \frac{\rho_d}{\rho_w} + LWC \tag{9}$$

where ε_s' is the real part of snow permittivity (unitless), ρ_d the dry snow density (kg m^{-3}), ρ_s the wet snow density (kg m^{-3}) and ρ_w the water density (kg m^{-3}). The theoretical accuracy of the wetness measurement is about ± 0.5% (Tiuri et al., 1982).

2.4. WISe resonator

The A2 Photonic Sensors' WISe (A2 Photonic Sensors, 2019) is composed of a metal cylinder with an inner central rod, the two components acting as a capacitor. The permittivity of the snow inside the instruments is evaluated from the resonant frequency of the system using a calibration equation not provided by the manufacturer. Since the WISe provides permittivity measurements, it is possible to use it for measuring LWC. Stein et al. (1997) validated empirical relationships to infer LWC from WISe measurements using calorimetry measurements as a reference and a methodology similar to that used for the Snow Fork (Sihvola and Tiuri, 1986). It probes a cylindrical encased snow sample of 5.5 × 13 cm. The time domain reflectometer is now a commercially produced instrument, and Eq. 10 is the current empirical relationship used to retrieve LWC from the real part of the measured snow with a measurement uncertainty of ± 1% LWC (A2 Photonic Sensors, 2019).

$$\varepsilon_s' = 1 + 1.202\left(\frac{\rho_d}{\rho_w} - LWC\right) + 0.983\left(\frac{\rho_d}{\rho_w} - LWC\right)^2 + 21.3LWC \tag{10}$$

2.5. Open-ended coaxial probe (OECP)

2.5.1. LWC retrieval from OECP measurements

An open-ended coaxial probe (OECP) was developed by the Université de Sherbrooke (UdeS) to monitor the permittivity and liquid water content of trees (Mavrovic et al., 2018). The very same OECP was used for the snow applications detailed in this paper, the calibration equations are presented in section 2.5.2. The OECP acts as a waveguide, therefore the reflection coefficient at the interface between its tip and

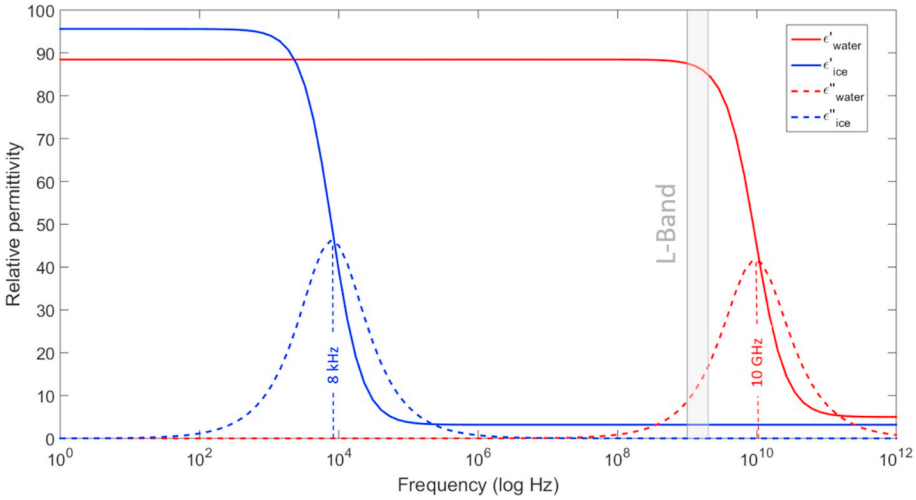

Fig. 2. Real (ε') and imaginary (ε'') parts of the relative permittivity (unitless) of water and ice at 273 K according to the Debye relaxation model (Mätzler, 1987; Artemov and Volkov, 2014).

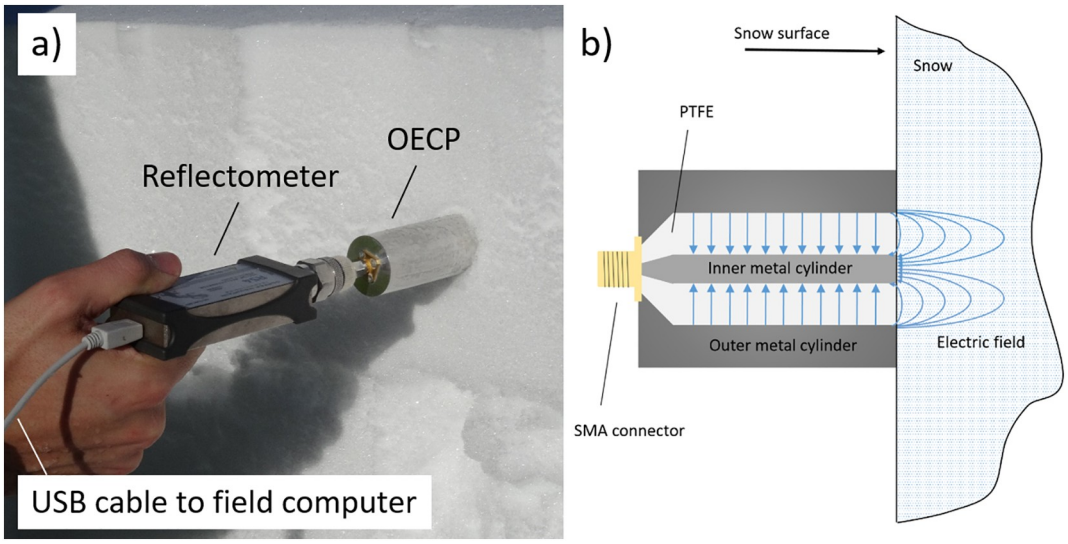

Fig. 3. (a) Open-ended coaxial probe kit for permittivity measurement. The manufacturer of the Planar R54 reflectometer provides the RVNA control program that can be operated by any field computer. To connect the probe to the Planar R54 reflectometer, an SMA/N cable or adaptor is required. (b) Diagram of the electrical field produced by the open-ended coaxial probe.

the probed medium is measured by a reflectometer connected to the OECP. The reflection coefficient of the probed medium depends on its permittivity, which is retrieved using a calibration based on an open (air), short (copper plate) and load (saline solutions of known permittivity) measurement. The OECP can provide the permittivity of a wide range of materials, and since it was developed to operate at L-band (1.4 GHz), it is sensitive to LWC because of the large dielectric contrast between liquid water, ice and air. While water permittivity has a strong dependency on frequency (Fig. 2), the value of the real part of ice permittivity is 3.17, over a large frequency range from 10 MHz to 1 THz and with a very slight temperature dependency (Mätzler and Wegmuller, 1987; Mätzler et al., 2006). The probed depth of the OECP depends on the penetration of the effective electric field generated by the probe, proportional to the permittivity of the medium (Fig. 3b). In fact, its frequency (1.4 GHz), makes the probed depth thinner than the other available instruments in the MHz range (see above sections) due to the loss factor (i.e. imaginary part of permittivity) larger at 1.4 GHz than it is at lower frequencies. The OECP penetration depth approaches 1 cm and the cylindrical probed volume is about 3 cm wide. The probe was developed with the requirement that it must be operational on field campaigns in remote environments. Therefore, the system is easily transportable, reasonably sized in terms of weight and dimensions, low energy consuming, operational at low temperatures and weatherproof. It also has a comparable in costs to the WISe (5000–7000 USD) and is substantially cheaper than a Snow Fork (11,000 USD). The OECP takes a permittivity measurement in less than a second once it is put in contact with the snow. In addition, the probe does not require destructive sampling of the snow wall although the user must take care to have a proper flat contact surface between the probe and the snow (Fig. 3a).

To the best of our knowledge, every operational modern method to obtain LWC in the field is based on the empirical relationship between LWC and permittivity and uses calorimetry measurements as the reference. The applicability and effectiveness of those empirical relationships are limited to the instrument they were developed for. In our case, we used a physically-based model to extract LWC from snow permittivity measurements of the OECP. Since snow is a mixture of ice, water and air, a simple way to theorize the snow permittivity (ε_s) is to use a simple mixing formula of the permittivity of the three constituents (Eq. 11) (Colbeck, 1982).

$$\varepsilon_s = f_i \varepsilon_i + f_w \varepsilon_w + f_a \varepsilon_a \quad (11)$$

where f_i, f_w and f_a are respectively fractions of ice, water and air in the snow following Eq. 12, while ε_i, ε_w and ε_a are respectively the ice, water and air permittivity.

$$f_i + f_w + f_a = 1 \quad (12)$$

Eq. 11 stands for both the real and imaginary parts of the permittivity. To add precision and complete our system of equations, we add the relationship between snow density (ρ_s) and the density of the ice, water and air that composed the snow (Eq. 13).

$$\rho_s = f_i \rho_i + f_w \rho_w + f_a \rho_a \quad (13)$$

Eq. 11 might be physically based, but theoretically does not account for the snow matrix (i.e. the snow microstructure geometry and inhomogeneity), which can affect its permittivity (Denoth, 1982). To resolve this issue, an empirical constant β is introduced in order to account for the snow matrix structure (Eq. 14) (Tiuri et al., 1982; Ulaby et al., 1986):

$$(\varepsilon_s)^\beta = f_i (\varepsilon_i)^\beta + f_w (\varepsilon_w)^\beta + f_a (\varepsilon_a)^\beta \quad (14)$$

2.5.2. OECP calibration

The OECP estimates the permittivity of a medium based on a calibration made on reference media. This calibration needs the measurement of defined parameters allowing the conversion of the reflection coefficient ρ, measured by the reflectometer, into the probed medium's permittivity. The medium permittivity can be obtained from its admittance Y (inverse of the impedance) by solving the following equation (Filali et al., 2006, 2008):

$$Y(\varepsilon) = \frac{2jk^2}{2\pi f \mu_o \left(ln\left(\frac{b}{a}\right)\right)^2} \int_a^b \int_a^b \int_0^\pi \frac{cos\varphi e^{-jkr}}{r} d\varphi du du' \quad (15)$$

where k is the wavenumber ($k = 2\pi f \sqrt{\varepsilon_r \varepsilon_o \mu_o}$) in radians per meter, $r = \sqrt{u^2 + u'^2 + 2uu' cos\varphi}$, f is the frequency in hertz, ε_r is the media relative permittivity, ε_o is the vacuum absolute permittivity, μ_o is the vacuum absolute permeability, (u, u',φ) are the cylindrical coordinates and a and b represent the internal and external radius of the coaxial probe in meters, respectively. Solving Eq. 15 numerically requires a vast amount of computing power because of integration singularities. For a much more effective calculation, the exponential term in Eq. 15 can be approximated by a Taylor series with subtle differences in results (Blackham and Pollard, 1997) leading to Eq. 16

$$Y(\varepsilon) = \frac{2jk^2}{2\pi f \mu_o \left(ln\left(\frac{b}{a}\right)\right)^2} \sum_{n=1}^{\infty} \frac{k^{n-1} I_n}{(n-1)!} \quad (16)$$

where

$$I_n = (-j)^{n-1} \int_a^b \int_a^b \int_0^\pi r^{n-2} cos\varphi d\varphi du du' \quad (17)$$

In this study, 50 Taylor series were used, while Filali et al. (2008) showed that 20 terms are needed for the Taylor series to converges. The admittance is linked to the probe voltage reflection coefficient Γ at the contact interface between the probe and the sample via Eq. 18 where Y_o represents the admittance of the probe ($Y_o = \frac{1}{50}\Omega^{-1}$) and $Y(\varepsilon)$ represents the admittance of the medium.

$$\Gamma = \frac{Y_o - Y(\varepsilon)}{Y_o + Y(\varepsilon)} \quad (18)$$

From there, Eq. 19 is used to retrieve the three unknown probe scattering parameters of the OECP (S_{11}, $S_{12}S_{21}$ and S_{22}) using at least three reference media with known reflection coefficients Γ (or the permittivity). Here we used an open circuit, a short circuit and a saline solution of known permittivity (Cole and Cole, 1941; Nyshadham et al., 1992) as reference media.

$$\Gamma = \frac{\rho - S_{11}}{S_{11}\rho + S_{12}S_{21} - S_{11}S_{22}} \quad (19)$$

The nonlinear equation system presented here to retrieve a medium permittivity was solved using a Levenberg-Marquardt Algorithm using the Gauss-Newton's method based on the least-square calculation.

3. Data and methods

3.1. Study sites

To obtain a wide range of LWC conditions, most of the data were acquired during the 2018 Rogers Pass campaign at the Mount Fidelity research site in Glacier National Park (British Columbia, Canada) from April 25th to May 2nd at the peak of the 2018 wet avalanche cycle. The site is the subject of ongoing snow research by Parks Canada and our group's avalanche program and is heavily instrumented with a long history of snow measurements going back to 1962 (Schleiss, 1990). Data were collected at the bottom of the valley near the Rogers Pass Discovery Centre (51°19′N, 117°31′W, 1330 m a.s.l.) and at the Mt. Fidelity alpine site (51°14′N, 117°70′W, 1880 m a.s.l.). To obtain dry snow measurements, data were collected in the Arctic circle at Trail Valley Creek (TVC), the research camp managed by Wilfrid Laurier University, 50 km north of Inuvik (Northwest Territories, Canada, 68°44′N, 133°28′W, 60 m a.s.l.) between the 19th and 27th of March 2019. To complete the database, measurements were also conducted at the SIRENE (Site Interdisciplinaire de Recherche en ENvironnement Extérieur, 45°22′N, 71°52′W, 305 m a.s.l.) research station of the Université de Sherbrooke (Québec, Canada) during a winter thaw event in December 2018.

3.2. Snow measurements

Vertical profile measurements of snow properties were conducted at all sites. Snowpack measurements were taken at 5 cm vertical intervals (3 cm for TVC) and included: snow temperature (T_{snow}, K), density (ρ_{snow}, kg·m^{-3}), specific surface area (SSA, m^2·kg^{-1}), grain extent (mm) and type. Snow density was obtained with a gravimetric approach (using a 250 cm^3 density cutter and samples weighed using a 100 g Pesola light series scale with an accuracy of 0.5 g). This traditional approach is estimated to provide a mean density accuracy of 5 to 9% (Proksch et al., 2016). SSA was obtained using an InfraRed Integrating Sphere (IRIS) described in detail in Montpetit et al. (2012).

In each snowpit, LWC data were acquired using calorimetry and the three available devices: Snow Fork, an early version of the WISe and OECP. The vertical spacing between measurements was a function of the probed volume for each instrument: 10 cm for the WISe, 5 cm for the OECP and 3 cm for the Snow Fork. There is no requirement on the snow sample for calorimetry besides that more snow reduces uncertainties. Therefore, a cylindrical snow cutter of dimensions 5.5 × 18 cm was used. Since LWC can vary significantly when the evaluated snow is exposed to ambient air, especially with warm temperature (i.e. > 0 °C), the LWC measurements were conducted simultaneously with the four instruments. For snowpits taller than two meters, the measurements were done in successive layers to reduce delay between exposing snow and measurements. In all cases, measurements were done from top to bottom and few centimeters of snow were removed from the snow wall before taking a measurement with the instruments horizontally oriented. The full set of measurements would usually take half an hour for one meter snow depth. Data used for performance evaluation (Sections 4.2 and 4.3) were performed on homogeneous layers of 10 cm thick or more. Table 1 presents the dates and sites where the full set of snow measurements were conducted in snowpits.

Table 1
Dates and location with air temperature (T_{air}), snow depth (d_{snow}) and number of snowpit (N).

Date	T_{air} (°C)	d_{snow} (cm)	N	Terrain type	Site
[26/04/2018–27/04/2018]	[4.6–6.1]	[139–149]	2	Valley in mountainous area	Rogers pass
[28/04/2018–01/05/2018]	[2.1–9.0]	322	3	Alpine	Fidelity
21/12/2018	6.3	40	1	Valley	SIRENE
[19/03/2019–27/03/2019]	[−18.0 – −7.9]	[18–65]	24	Arctic	TVC

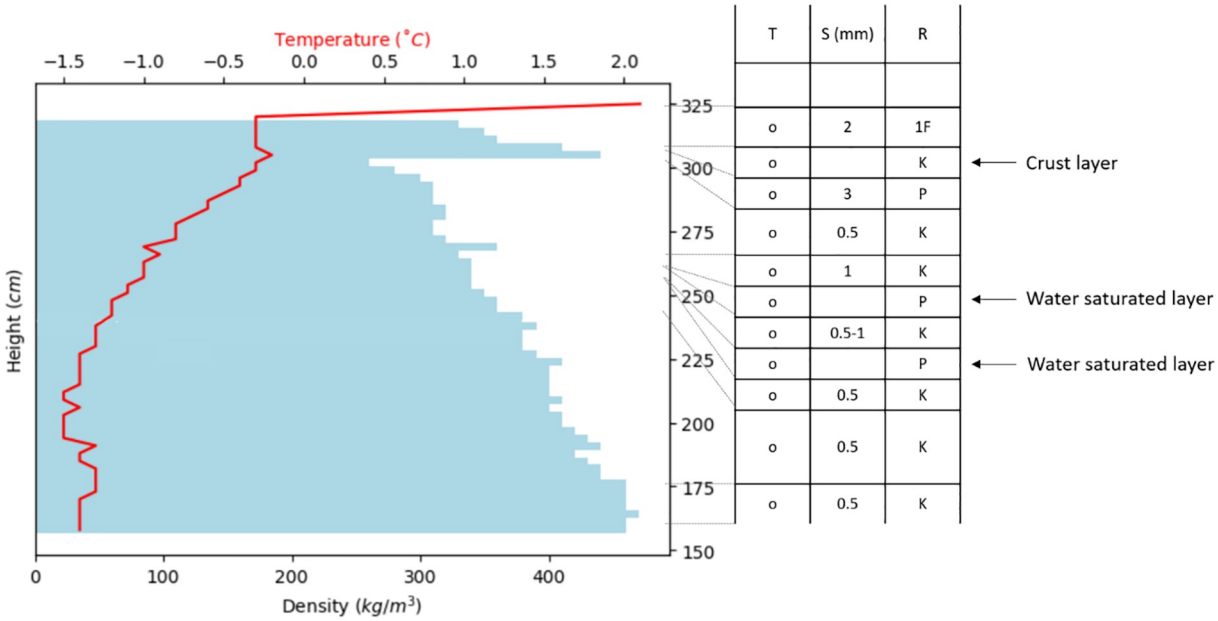

Fig. 4. Physical properties of the snowpack profile on May 30th 2018 at the Mt. Fidelity alpine site. *T* represents the grain type according to the classification of Fierz et al. (2009), *o* is the symbol for melt form grains. *S* represents the grain size in mm as observed through a magnifying glass. *R* represents the resistance or hardness of the snow evaluating qualitatively depending on the size of the biggest shape easily passing through the snow: fist (F), one finger (1F), four fingers (4F), pen (P) or knife (K) (Fierz et al., 2009).

4. Results

4.1. Snowpack physical properties

Fig. 4 displays vertical profiles of snow physical properties for an alpine snowpack on May 30th 2018, used to evaluate the LWC profile (Fig. 8). This profile is representative of the snowpack observed throughout the 2018 Rogers Pass campaign.

4.2. LWC extraction from OECP measurements

Of all the available empirical relationships developed to link LWC to permittivity, the relationship developed for the Snow Fork by Tiuri et al. (1984) is closest in frequency to the OECP (Eq. 7). While applied to OECP data, this empirical relationship highly overestimates LWC (Fig. 5) compared to calorimetry measurements and typical expected values. Even when the snow density information is added to the Snow Fork (Eq. 8), the LWC overestimation persists. It seems that although the Tiuri et al. (1984) relationship works well with Snow Fork permittivity values (below 1 GHz), it is not applicable to L-band measurements. One should also note that the permittivity of liquid water starts to drop at around 1 GHz (Fig. 2). Good agreement was found between calorimetry and OECP measurements when the simple mixing formula (Eq. 11, 12 and 13) was used to extract LWC. This snow permittivity model is physically based and has the advantage of being independent of any empirical relationship.

4.3. Performance evaluation

The LWC was evaluated using four different techniques: OECP, Snow Fork, WISe and calorimetry. Homogeneous thick snow layers of different LWC were selected to provide a common evaluation reference for all techniques. With calorimetry measurements set as the reference technique, all three other techniques showed good agreement with root mean square error (RMSE) of 1.00% (OECP), 1.26% (Snow Fork) and 1.33% (WISe) (Fig. 6). This corroborates the results of Techel et al. (2011). In this regard, the OECP proved to be a suitable technique for LWC, displaying similar precision to the Snow Fork and WISe instruments.

In order to evaluate the impact of snow microstructure on OECP retrieval, the RMSE between the OECP and calorimetric LWC was minimized to optimize the fitting parameter β of Eq. 14 (Fig. 7). β converged to a value close to 1, therefore no improvements were integrated by using Eq. 14 instead of Eq. 11.

To validate OECP measurements, the probe was frozen in a block of ice. Ice permittivity measurement with the OECP gave 3.04 ± 0.01, which is slightly less than the theoretical value of 3.17 for ice at -15 °C (temperature at which $\varepsilon_{ice\ OECP}$ was obtained) (Mätzler and Wegmuller, 1987). This underestimation can be attributed to the difficulty to have pure ice without any air infiltration, as the ice density and permittivity decreasing with air presence (Mätzler and Wegmuller, 1987; Fujita et al., 2000). Although the block of ice displayed no visible air bubbles or cloudiness, no purity testing was conducted on the ice.

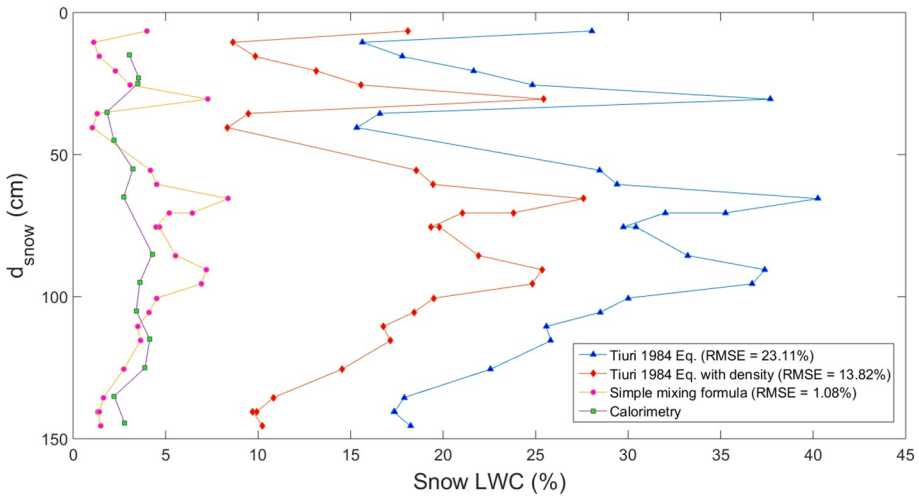

Fig. 5. LWC (% of volume) profile at Fidelity research site on May 26th 2018 using the OECP. The LWC at various snow depths (d_{snow}) was calculated from OECP permittivity using Tiuri et al. (1984) equations (blue triangle), Tiuri et al. (1984) equations with independent density information (orange diamond), the simple mixing formula (pink circle). Calorimetry data are given as the reference data (green circle). Root-Mean-Square Error (RMSE) is given in parentheses with calorimetry as the reference data. (For interpretation of the references to colour in this figure legend, the reader is referred to the web version of this article.)

4.4. LWC measurement techniques comparison

The smaller probed volume of the OECP compared to the other available LWC instruments gives a higher vertical resolution. Fig. 8 displayed a snowpack vertical profile during a thawed event where two thin layers with high LWC were visually observed at 37 and 56 cm depth. Those layers are the result of water accumulation on dense layers during percolation processes. The vertical resolution of the OECP shows to be sensitive enough to capture the high LWC of those layers. For very wet snow, LWC over 8% is expected (Techel and Pielmeier, 2011) which is in agreement with the OECP results. Sadiku (1985) also evaluated wet snow to be over 7% and "watery" snow to be over 25% of LWC. Other instruments were not able to detect them or underestimated the LWC fluctuations near those critical layers in the snowpack owing to a sample volume significantly larger than the layer thickness. Therefore, the high LWC layer does not have enough weight on the averaged LWC measurement over the probed volume.

4.5. Dry snow density

Dry snow measurements were also performed with the OECP in order to improve the confidence in the snow permittivity measurements. The relationship between permittivity and dry snow density is displayed in Fig. 9. This relationship is expected because ice permittivity is slightly higher than air permittivity (Fig. 2). Since the dielectric contrast between air and ice is lower than between water and air/ice, the relationship between permittivity and dry density is not as strong as with LWC. As shown in Fig. 9, the coefficient of determination of the linear regression between permittivity and dry density is 0.66. The dry snow density can be calculated using Eq. 11 through 13, assuming that when the snow is dry, $f_w = 0$. The results are shown in Fig. 10. The precision can be estimated using the RMSE of 79.8 kg·m^{-3} (> 20%) between the calculated and measured (density cutter) dry snow density. The OECP displays a systematic underestimation of dry snow density. The OECP precision for dry snow density is lower than with the classical density cutter method because the dielectric contrast between ice and air is small. This held true for other methods using permittivity for dry snow density evaluation.

5. Discussion

The OECP precision is similar to other indirect measurement instruments that use microwave permittivity, which stands around ± 1% LWC. However, the OECP shown to be more suitable to capture and quantify thin percolation accumulation layers (few cm) in the snowpack. The characterization of those thin layers is critical for the validation of percolation models and avalanche risk assessments. This improved capability is due to a smaller probed volume (3 × 3 × 1 cm). However, it should be kept in mind that the smaller probed volume makes the OECP more sensitive to inhomogeneity in the snowpack. Table 2 gives an overview of the main pros and cons of the studied available LWC instruments.

It must be pointed out that the development of the OECP relies on using calorimetry measurements as the reference method, despite the fact that calorimetry also bears some uncertainties due to the sensitivity of the methodology and the heat lost during the mixing of snow and

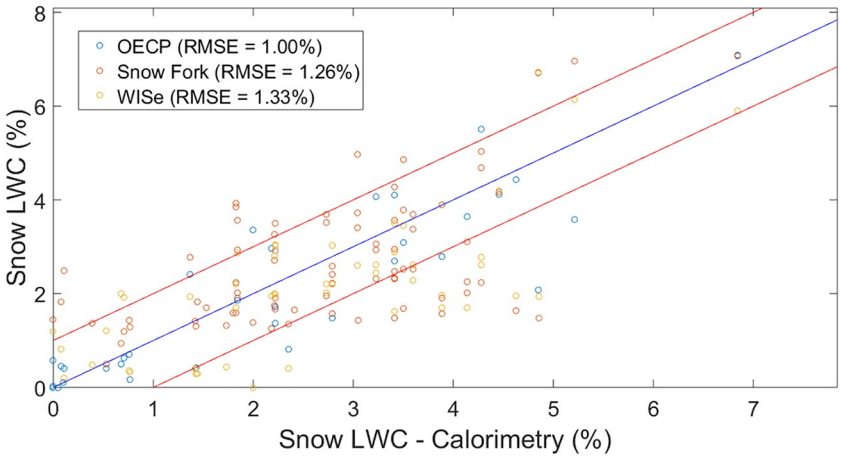

Fig. 6. Comparison of LWC (% of volume) obtained with three independent techniques with calorimetry measurements as the reference. All data were acquired at the Fidelity research site between May 26th and April 2nd 2018 ($N = 90$). RMSE is given in parentheses with calorimetry as the reference data. The blue line represents the perfect fit between permittivity-inferred LWC and calorimetric reference data. The red line is the typical ± 1% precision of LWC. The coefficient of determination is 0.66 for the OECP, 0.29 for the Snow Fork and 0.45 for the WISe. (For interpretation of the references to colour in this figure legend, the reader is referred to the web version of this article.)

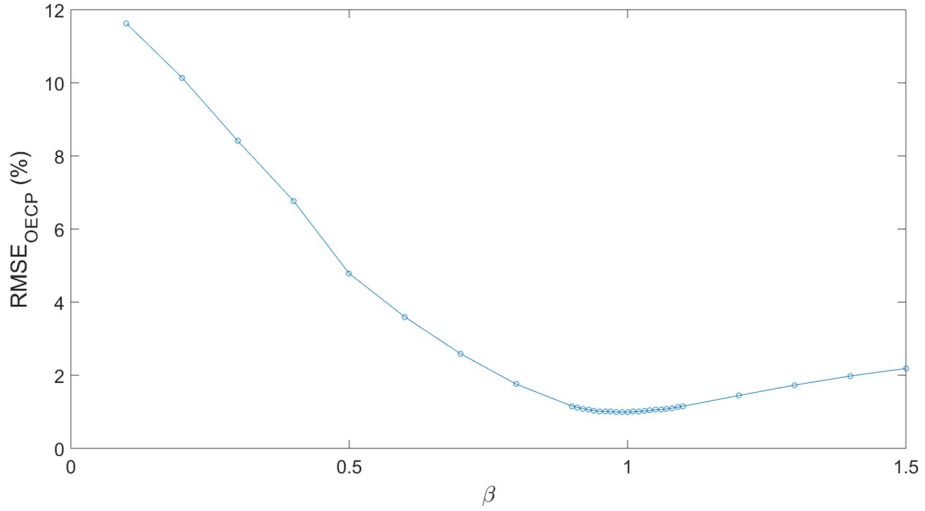

Fig. 7. Fitting of the β parameter, Eq. 14. The RMSE is calculated between the OECP and the calorimetric data from Fig. 6.

water. That consideration does not differ from other permittivity-based devices for LWC since they all rely on calorimetry measurements for calibration.

Since the values of the fitting parameter β converges to approximately 1, Eq. 11 and 14 provided the same results. Tiuri et al. (1982) proposed that β could be related to the snow matrix structure: type of snow grain and SSA or size. The LWC data presented in this study were acquired on melt form grains, a common grain type for wet snow. Other grain types, such as hoar grains, can be observed in wet conditions, and it should thus be kept in mind that the optimized β could differ for these other grain types.

Satellite-based microwave radiation is one of the main ways to monitor snow physical properties over vast regions (Kinar and Pomeroy, 2015). However, the presence of liquid water in the snow radically increases the absorption of microwaves and consequently greatly reduces the penetration depth (of the order of 1 cm at 19 and 37 GHz). Even a few percent of liquid water content efficiently absorbs microwaves (Pomerleau et al., 2019; Picard et al., 2013). While it is possible to detect wet snow using emitted microwaves or backscattered signals (Appel et al., 2019; Brucker et al., 2011; Royer et al., 2010; Koskinen et al., 2010; Marshall et al., 2004; Fierz et al., 2009; Tedesco et al., 2006; Rawlins et al., 2005), a better understanding of the interaction between microwaves and wet snow is required to obtain a LWC retrieval algorithm from microwaves, which already show great potential at L-band (Naderpour and Schwank, 2018).

Due to the small probed volume and thus high vertical resolution, the OECP probe could also be an important tool for the development and the validation of fixed radar measurements of snow cover properties. Recent years have seen an increasing number of radar research for applications in avalanche risk assessments (Pasian et al., 2019). The radar signal becomes difficult to evaluate in the presence of LWC in the snowpack (Okorn et al., 2014; Mitterer et al., 2011b). The measurement of snow dielectric properties with good precision is important to understand how the wet snow influences the signal (Marshall et al., 2004). Schmid et al., 2016were able to derive a bulk quantification of LWC combining ground penetrating radar (GPR) and GPS data. They compared their radar measurements with the Snow Fork and Denoth instruments showing agreement but the high variability in the dielectric data measurements from both devices made the comparison difficult. A less destructive approach with the OECP could help obtain more precise information on the LWC and the dielectric characteristics of the evaluated snowpack.

The OECP has been previously shown to be a suitable device for monitoring the permittivity of trees (Mavrovic et al., 2018). Those data

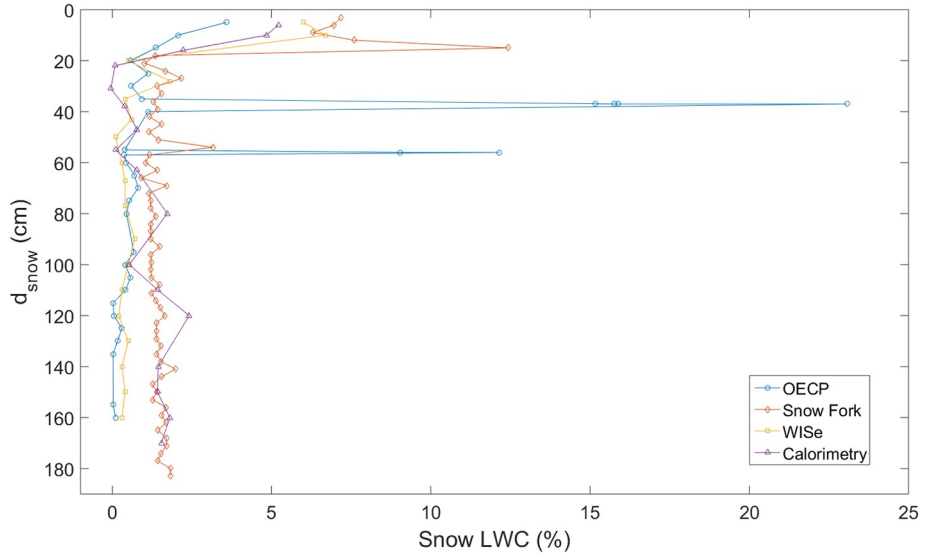

Fig. 8. LWC (% of volume) profile at Fidelity research site on May 30th 2018 measured with four different techniques. LWC fluctuated through snow depth (d_{snow}).

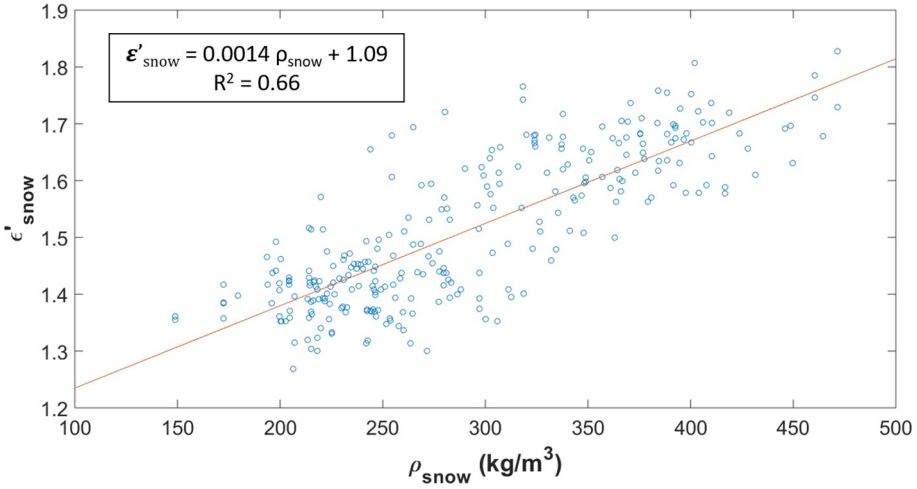

Fig. 9. Relationship between dry snow permittivity (ε'_{snow}) and snow density (ρ_{snow}). All data were acquired at the TVC research site between March 19th and 27th 2019 (blue dots, $N = 284$) with temperature below -10 °C. The linear regression (red line) parameters is given in legend with the coefficient of correlation (R^2). (For interpretation of the references to colour in this figure legend, the reader is referred to the web version of this article.)

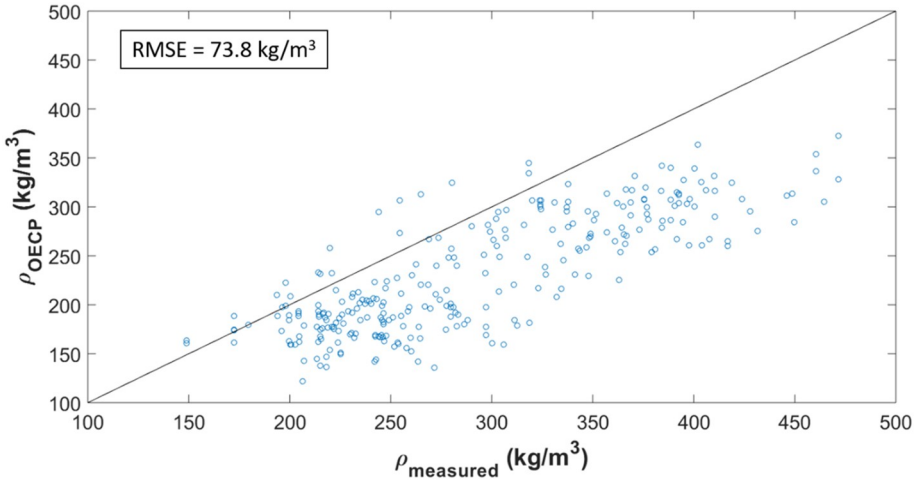

Fig. 10. Comparison of the snow density obtained with the OECP (ρ_{OECP}) and measured with a density cutter ($\rho_{measured}$). All data were acquired at the TVC research site between March 19th and 27th 2019 (blue dots, N = 284). (For interpretation of the references to colour in this figure legend, the reader is referred to the web version of this article.)

Table 2
Pros and cons of four different LWC measurement methods.

	OECP	Snow Fork	TDR	Calorimetry
Pros	• Small probed volume • Quick measurement • Transportable	• Quickest measurement • Transportable	• Quick measurement • Most transportable • Defined probed volume	• Reference method based on direct snow LWC measurement • Scalable probed volume
Cons	• Sensitive to inhomogeneity • Requires a flat contact with snow	• Only for snow LWC < 10% • Snow compaction • Variable, not clearly defined and large probed volume • Most expensive	• Only for snow LWC < 10% • Snow compaction • Required independant density measurements • Large probed volume	• Requires a lot of material • Hard to transport • Time-consuming

on trees are useful both for microwave radiative transfer modeling through the canopy and monitoring tree hydrologic processes. Also, the OECP showed great potential to monitor soil permittivity (Mavrovic et al., in progress). There are great benefits to a multifunctional probe that can be used for snow, soil and vegetation, notably for calibrating and validating microwave radiative transfer models.

6. Conclusions

This paper showed that the open-ended coaxial probe (OECP) is a suitable device for measuring LWC in snow. The OECP device that was developed displayed uncertainties of ± 1% of LWC when compared to the calorimeter method considered as a reference LWC measurement. This precision is similar to other available instruments such as the Snow Fork and the WISe. The OECP also proved to have a probed volume small enough to capture the LWC of thin percolation accumulation layers, which other instruments failed to do due to their lower frequencies. This study also proved that a simple physically-based mixing model can be used to infer LWC from L-band microwave permittivity. However, this model might be impacted by snow microstructure and could be improved by accounting for the snow matrix (i.e. grain size and type). Future work will look at the impact of grain size and type on the LWC retrieval algorithm with the OECP in L-band and at higher frequencies (10 GHz).

Data availability

The research data is available upon request.

Declaration of Competing Interest

The authors declare that they have no known competing financial interests or personal relationships that could have appeared to influence the work reported in this paper.

Acknowledgments

This work was made possible thanks to the contributions of the Canadian Space Agency (CSA), the Natural Sciences and Engineering Research Council of Canada (NSERC), the Canada Foundation for Innovation (CFI) and the Search and Rescue New Initiatives Fund (SARNIF). A special thanks to Jeff Goodrich and his team at Parks Canada for providing logistical support in the field and making it possible for us to safely collect data in avalanche terrain. We would also like to thank Dr. Bilal Filali for his contribution in the design and manufacturing of the probe, Prof. Patrick Ayotte (University of Sherbrooke) and his student Clément Wespiser for their help with the calorimetry protocol, Claude Duguay (University of Waterloo) for providing the SnowFork instrument, Michel Fily (Institut des géosciences et de l'environnement of Grenoble) for providing the WISe instrument, Prof. Philip Marsh (Wilfrid Laurier University) for providing logistical support at the TVC research site as well as everyone who helped on the field for all the campaigns: Prof. Dr. Nick Rutter (Northumbria University), Prof. Richard Essery (Edinburgh University), PhD Joshua King (Environment and Climate change Canada, ECCC), Peter Toose (ECCC), Arvids Silis (ECCC), Branden Walker (Wilfrid Laurier University) and Jacob Laliberté (Université de Sherbrooke). Finally, we would like to recognize the reviewers who improved the paper by their useful comments.

References

A2 Photonic Sensors, 2019. WISe – Snow liquid water content sensor – User manual. In: A2 Photonic Sensors, Grenoble, France, (10 pages).
Aebischer, H., Maetzler, C., 1983. A microwave sensor for the measurement of the liquid water content on the surface of the snow cover. In: 13th European Microwave Conference Proceedings. IEEE, pp. 483–487.
Appel, F., Koch, F., Rösel, A., Klug, P., Henkel, P., Lamm, M., Mauser, W., Bach, H., 2019. Advances in Snow Hydrology Using a Combined Approach of GNSS in Situ Stations, Hydrological Modelling and Earth Observation—A Case Study in Canada. Geosciences. 9(1). pp. 44.
Artemov, V., Volkov, A., 2014. Water and ice dielectric spectra scaling at 0 °C. Ferroelectrics 466 (1), 158–165.
Barrere, M., Dominé, F., Belke-Brea, M., Sarrazin, D., 2018. Snowmelt events in Autumn can Reduce or Cancel the Soil Warming effect of Snow–Vegetation Interactions in the Arctic. J. Clim. 31 (23), 9507–9518.
Blackham, D., Pollard, R., 1997. An improved technique for permittivity measurements using a coaxial probe. IEEE Trans. Instrum. Meas. 46 (5), 1093–1099.
Brucker, L., Royer, A., Picard, G., Langlois, A., Fily, M., 2011. Hourly simulations of the microwave brightness temperature of seasonal snow in Quebec, Canada, using a coupled snow evolution-emission model. Remote Sens. Environ. 115 (8), 1966–1977.
Colbeck, S.C., 1982. The geometry and permittivity of snow at high frequencies. J. Appl. Phys. 53 (6), 4495–4500.
Cole, K., Cole, R., 1941. Dispersion and absorption in dielectrics - Alternating current characteristics. J. Chem. Phys. 9, 341–351.
D'Amboise, C.J.L., Müller, K., Oxarango, L., Morin, S., Schuler, T.V., 2017. Implementation of a physically based water percolation routine in the Crocus (V7) snowpack model. Geosci. Model Dev. 10, 3547–3566.
Denoth, A., 1982. Effect of grain geometry on electrical properties of snow at frequencies up to 100 MHz. J. Appl. Phys. 53 (10), 7496–7501.
Denoth, A., 1989. Snow dielectric measurements. Adv. Space Res. 9 (1), 233–243.
Denoth, A., 1994. An electronic device for long-term snow wetness recording. International Glaciological Society 19, 105–106.
Denoth, A., Foglar, A., Weiland, P., Mätzler, C., Aebischer, H., Tiuri, M., Sihvola, A., 1984. A comparative study of instruments for measuring the liquid water content of snow. J. Appl. Phys. 56 (7), 2154–2160.
Derksen, C., Xu, X., Dunbar, R.S., Colliander, A., Kim, Y., Kimball, J., Black, A., Euskirchen, E., Langlois, A., Loranty, M., Marsh, P., Rautiainen, K., Roy, A., Royer, A., 2017. Retrieving landscape freeze/thaw state from Soil Moisture active Passive (SMAP) radar and radiometer measurements. Remote Sens. Environ. 194, 48–62.
Dolant, C., Langlois, A., Brucker, L., Royer, A., Roy, A., Montpetit, B., 2017. Meteorological inventory of rain-on-snow events in the Canadian Arctic Archipelago and satellite detection assessment using passive microwave data. Phys. Geogr. 45 (10), 4908–4916.
Dolant, C., Montpetit, B., Langlois, A., Brucker, L., Zolina, O., Johnson, C.A., Royer, A., Smith, P., 2018. Assessment of the Barren Ground Caribou Die-off during Winter 2015–2016 using Passive Microwave Observations. Geophys. Res. Lett. 45 (10), 4908–4916.
Dominé, F., Albert, M., Huthwelker, T., Jacobi, H.-W., Kokhanovsky, A.A., Lehning, M., Picard, G., Simpson, W.R., 2008. Snow physics as relevant to snow photochemistry. Atmos. Chem. Phys. 8 (2), 171–208.
Entekhabi, D., Njoku, E., O'Neill, P., Kellogg, K., Crow, W., Edelstein, W., Entin, J., Goodman, S., Jackson, T., Jackson, J., Kimball, J., Piepmeier, J., Koster, R., Martin, N., McDonald, K., Moghaddam, M., Moran, S., Reichle, R., Shi, J., Spencer, M., Thurman, S., Tsang, L., Van Zyl, J., 2010. The Soil Moisture active Passive (SMAP) mission. Proc. IEEE 98, 704–716.
Fierz, C., Armstrong, R.L., Durand, Y., Etchevers, P., Greene, E., McClung, D.M., Nishimura, K., Satyawali, P.K., Sokratov, S.A., 2009. The International Classification for Seasonal Snow on the Ground. In: IHP-VII Technical Documents in Hydrology N°83, IACS Contribution N°1. UNESCO-IHP, Paris (80 pages).
Filali, B., Rhazi, J.-E., Ballivy, G., 2006. Measurement of the dielectric properties of concrete by a large coaxial probe with open end. Can. J. Phys. 84 (5), 365–379.
Filali, B., Boone, F., Rhazi, J.-E., Ballivy, G., 2008. Design and calibration of a large open-ended coaxial probe for the measurement of the dielectric properties of concrete. IEEE Transactions on Microwave Theory and Techniques 56 (10), 2322–2328.
Fujita, S., Matsuoka, T., Ishida, T., Matsuoka, K., Mae, S., 2000. A summary of the complex dielectric permittivity of ice in the megahertz range and its applications for radar sounding of polar ice sheets. In: Physics of ice core Records. Hokkaido University Press, Sapporo, Japan, pp. 185–212.
Jones, E.B., Rango, A., Howell, S., 1983. Snowpack liquid water determinations using freezing calorimetry. Nord. Hydrol. 14, 113–126.
Kendra, J., Ulaby, F., Sarabandi, K., 1994. Snow Probe for *In Situ* Determination of Wetness and Density. IEEE Trans. Geosci. Remote Sens. 32 (6), 1152–1159.
Kerr, Y.H., Waldteufel, P., Wigneron, J.P., Delwart, S., Cabot, F.O., Boutin, J., Escorihuela, M.J., Font, J., Reul, N., Gruhier, C., Juglea, S.E., 2010. The SMOS mission: New tool for monitoring key elements of the global water cycle. IEEE Trans. Geosci. Remote Sens. 98, 666–687.
Kinar, N.J., Pomeroy, J.W., 2015. Measurement of the physical properties of the snowpack. Rev. Geophys. 53 (2), 481–544.
Koskinen, J.T., Pulliainen, J.T., Luojus, K.P., Takala, M., 2010. Monitoring of Snow-Cover Properties during the Spring Melting Period in Forested areas. IEEE Trans. Geosci. Remote Sens. 48 (1), 50–58.
Langlois, A., Johnson, C.-A., Montpetit, B., Royer, A., Blukacz-Richards, E.A., Neave, E., Dolant, C., Roy, A., Arhonditsis, G., Kime, D.-K., Kaluskar, S., Brucker, L., 2017. Detection of rain-on-snow (ROS) events and ice layer formation using passive microwave radiometry: a context for Peary caribou habitat in the Canadian Arctic. Remote Sens. Environ. 189, 84–95.
Le Vine, D.M., Lagerloef, G.S., Torrusio, S., 2010. Aquarius and remote sensing of sea surface salinity from space. Proc. IEEE 98, 688–703.
Lundberg, A., 1997. Laboratory calibration of TDR-probes for snow wetness measurements. Cold Reg. Sci. Technol. 25 (3), 197–205.
Marshall, H.P., Koh, G., Forster, R.R., 2004. Ground-based frequency-modulated continuous wave radar measurements in wet and dry snowpacks, Colorado, USA: an analysis and summary of the 2002-03 NASA CLPX data. Hydrol. Process. 18 (18), 3609–3622.
Mätzler, C., 1987. Applications of the interaction of microwaves with the natural snow cover. Remote Sens. Rev. 34 (2), 573–581.
Mätzler, C., 1996. Microwave permittivity of dry snow. IEEE Trans. Geosci. Remote Sens. 48 (1), 50–58.
Mätzler, C., Wegmuller, U., 1987. Dielectric properties of freshwater ice at microwave frequencies. J. Appl. Phys. 20 (12), 1623.
Mätzler, C., Wiesmann, A., 2007. Documentation for MEMLS, Version 3 - Microwave Emission Model of Layered Snowpacks. Institute of Applied Physics - University of Bern, Bern (25 pages).
Mätzler, C., Rosenkranz, P.W., Battaglia, A., Wigneron, J.P., 2006. Thermal Microwave Radiation: Applications for Remote Sensing. Vol. 52. Institute of Engineering and Technology, Stevenage, United Kingdom, pp. 455–462 Chapter 5.
Mavrovic, A., Roy, A., Royer, A., Filali, B., Boone, F., Pappas, C., Sonnentag, O., 2018. Dielectric characterization of vegetation at L band using an open-ended coaxial probe. Geoscientific Instrumentation Methods and Data Systems 7, 195–208.
Mitterer, C., Hirashima, H., Schweizer, J., 2011a. Wet-snow instabilities: Comparison of measured and modeled liquid water content and snow stratigraphy. Ann. Glaciol. 52 (58), 201–208.
Mitterer, C., Heilig, A., Schweizer, J., Eisen, O., 2011b. Upward-looking ground-penetrating radar for measuring wet-snow properties. Cold Reg. Sci. Technol. 69 (2–3), 129–138.
Montpetit, B., Royer, A., Langlois, A., Cliche, P., Roy, A., Champollion, N., Picard, G., Dominé, F., Obbard, R., 2012. New shortwave infrared albedo measurements for snow specific surface area retrieval. J. Glaciol. 58 (211), 941–952.
Morin, S., Dominé, F., Arnaud, L., Picard, G., 2010. In-situ monitoring of the time evolution of the effective thermal conductivity of snow. Cold Reg. Sci. Technol. 64 (2), 73–80.
Naderpour, R., Schwank, M., 2018. Snow Wetness Retrieved from L-Band Radiometry. Remote Sens. Environ. 10 (3), 359.
Nyshadham, A., Sibbald, C., Stuchly, S., 1992. Permittivity measurements using open-ended sensors and reference liquid calibration - an uncertainty analysis. IEEE Transactions on microwave theory and techniques 40 (2), 305–314.
Okorn, R., Brunnhofer, G., Platzer, T., Heilig, A., Schmid, L., Mitterer, C., Schweizer, J., Eisen, O., 2014. Upward-looking L-band FMCW radar for snow cover monitoring. Cold Reg. Sci. Technol. 103, 31–40.

Pasian, M., Barbolini, M., Dell'Acqua, F., Espin-Lopez, P.F., Silvestri, L., 2019. Snowpack monitoring using a Dual-Receiver Radar Architecture. IEEE Trans. Geosci. Remote Sens. 57 (2), 1195–1204.
Pérez Diaz, C.L., Muñoz, J., Lakhankar, T., Khanbilvardi, R., Romanov, P., 2017. Proof of concept: Development of snow liquid water content profiler using CS650 reflectometers at Caribou, ME, USA. Sensors 17 (3) Switzerland.
Picard, G., Brucker, L., Roy, A., Dupont, F., Fily, M., Royer, A., Harlow, C., 2013. Simulation of the microwave emission of multi-layered snowpacks using the Dense Media Radiative transfer theory: the DMRT-ML model. Geosci. Model Dev. 6, 1061–1078.
Pomerleau, P., Royer, A., Cliche, P., Courtemanche, B., Langlois, A., 2019. Measuring Lake Ice Thickness and Snow Water Equivalent Using a Frequency-Modulated Continuous-Wave Radar. Cold Regions Science and Technology (Submitted).
Prince, M., Roy, A., Brucker, L., Royer, A., Kim, Y., Zhao, T., 2018. Northern hemisphere surface freeze/thaw product from Aquarius L-band radiometers. Earth System Science Data 10, 2055–2067.
Proksch, M., Rutter, N., Fierz, C., Martin, S., 2016. Intercomparison of snow density measurements: bias, precision, and vertical resolution. Cryosphere 10 (1), 371–384.
Rautiainen, K., Parkkinen, T., Lemmetyinen, J., Schwank, M., Wiesmann, A., Ikonen, J., Derksen, C., Davydov, S., Davydova, A., Boike, J., Langer, M., Drusch, M., Pulliainen, J., 2016. SMOS prototype algorithm for detecting autumn soil freezing. Remote Sens. Environ. 180, 346–360.
Rawlins, M., Mcdonald, K., Frolking, S., Lammers, R., Fahnestock, M., Kimball, J., Vorosmarty, C., 2005. Remote sensing of snow thaw at the pan-Arctic scale using the sea winds scatterometer. J. Hydrol. 312 (1–4), 294–312.
Roy, A., Toose, P., Williamson, M., Rowlandson, T., Derksen, C., Royer, A., Lemmetyinen, J., Berg, A., Arnold, L., 2017. Response of L-Band brightness temperatures to freeze/thaw and snow dynamics in a prairie environment from ground-based radiometer measurements. Remote Sens. Environ. 191, 67–80.
Royer, A., Goïta, K., Kohn, J., DeSève, D., 2010. Monitoring dry, wet and no- snow conditions from microwave satellite observations. IEEE Geosci. Remote Sens. Lett. 7 (4), 670–674.
Sadiku, M., 1985. Refractive index of snow at microwave frequencies. Appl. Opt. 24 (4), 572–575.
Schleiss, V.G., 1990. Rogers Pass Snow Avalanche Control - A Summary, Glacier National Park, British Columbia, Canada. Canadian Parks Service, Revelstoke, British Columbia, Canada (22 pages).
Schmid, L., Schweizer, J., Bradford, J., Maurer, H., 2016. A synthetic study to assess the applicability of full-waveform inversion to infer snow stratigraphy from upward-looking ground-penetrating radar data. Geophysics 81 (1), WA213–WA223.
Sihvola, A., Tiuri, M., 1986. Snow Fork for Field Determination of the Density and Wetness Profiles of a Snow Pack. IEEE Trans. Geosci. Remote Sens. GE-24 (5), 717–721.
Stein, J., Kane, D., 1983. Monitoring the Unfrozen Water Content of Soil and Snow using Time Domain Reflectometry. Water Resour. Res. 19 (6), 15733–15784.
Stein, J., Laberge, G., Lévesque, D., 1997. Measuring the dry density and the liquid water content of snow using time domain reflectometry. Cold Reg. Sci. Technol. 25, 123–136.
Takala, M., Luojus, K., Pulliainen, J., Derksen, C., Lemmetyinen, J., Kärnä, J.-P., Koskinen, J., 2011. Estimating Northern Hemisphere snow water equivalent for climate research through assimilation of space-borne radiometer data and ground-based measurements. Remote Sens. Environ. 115, 3517–3529.
Techel, F., Pielmeier, C., 2011. Point observations of liquid water content in wet snow - investigating methodical, spatial and temporal aspects. Cryosphere 5 (2), 405–418.
Tedesco, M., Kim, E., England, A., de Roo, R., Hardy, J., 2006. Observations and modeling of snow melting/refreezing cycles using a multi-layer dense medium theory-based model. IEEE Trans. Geosci. Remote Sens. 44, 3563–3573. https://doi.org/10.1109/TGRS.2006.881759.
Tiuri, M., Sihvola, A., Nyfors, E., 1982. Microwave sensor for snowpack wetness and density profile measurement. In: 1982 12th European Microwave Conference Proceedings, pp. 157–160.
Tiuri, M., Sihvola, A., Nyfors, E., Hallikaiken, M., 1984. The complex dielectric constant of snow at microwave frequencies. IEEE J. Ocean. Eng. OE-9 (5), 377–382.
Ulaby, F., Moore, R., Fing, A., 1986. Microwave Remote Sensing: Active and Passive, Volume 3. Artech House, Norwood, MA, United States.
Wever, N., Fierz, C., Mitterer, C., Hirashima, H., Lehning, M., 2014. Solving Richards Equation for snow improves snowpack meltwater runoff estimations in detailed multi-layer snowpack model. Cryosphere 8 (1), 257–274.
Wever, N., Vera Valero, C., Fierz, C., 2016a. Assessing wet snow avalanche activity using detailed physics based snowpack simulations. Geophys. Res. Lett. 43 (11), 5732–5740.
Wever, N., Urzer, S., Fierz, C., Lehning, M., 2016b. Simulating ice layer formation under the presence of preferential flow in layered snowpacks. Cryosphere 10, 2731–2744.
Yosida, Z., 1960. A calorimeter for measuring the free water content of wet snow. J. Glaciol. 3, 574–576.